Experimental studies of particle removal and probability of COVID-19 infection in passenger railcars

Darpan Das[*],

Kelsey R. Babik[*],

Emma Moynihan,

Gurumurthy Ramachandran

Department of Environmental Health and Engineering, Bloomberg School of Public Health, Johns Hopkins University, Baltimore, Maryland

Abstract

A series of experiments in stationary and moving passenger railcars was conducted to measure the removal rates of particles in the size ranges of SARS-CoV-2 viral aerosols, and the air changes per hour provided by the existing and modified air handling systems. The effect of ventilation and air filtration systems on removal rates and their effects on estimated probability (i.e., risk) of infection was evaluated in a range of representative conditions: (1) for two different ratios of recirculated air (RA) to outdoor air (OA) (90:10 RA:OA and 67:33 RA:OA); (2) using minimum efficiency reporting value (MERV) filters with standard (MERV-8) and increased (MERV-13) filtration ratings; and (3) in the presence and absence of a portable high-efficiency particulate-air (HEPA) room air purifier system operated at clean air delivery rate (CADR) of 150 and 550 cfm. The higher-efficiency MERV-13 filters significantly increased particle removal rates on average by 3.8 to 8.4 hr^{-1} across particle sizes ranging from 0.3 to 10 μm ($p < 0.01$) compared to MERV-8 filters. The different RA:OA ratios and the use of a portable HEPA air purifier system had little effect on particle removal rates. MERV-13 filters reduced the estimated probability of infection by 42% compared to the MERV-8 filter. The use of a HEPA-air purifier with a MERV-13 filter causes a 50% reduction in the estimated probability of infection. Upgrading the efficiency of HVAC filters from MERV-8 to MERV-13 in public transit vehicles is the most effective exposure control method resulting in a clear reduction in the removal rates of aerosol particles and the estimated probability of infection.

Keywords

CONTACT Gurumurthy Ramachandran gramach5@jhu.edu Department of Environmental Health and Engineering, Bloomberg School of Public Health, Johns Hopkins University, 615 N Wolfe St E6628, Baltimore, MD 21205, USA.
[*]These authors contributed equally to the manuscript.

Introduction

With the pandemic caused by the SARS-CoV-2 virus, commuters started working remotely during spring 2020 (WHO, 2021), and leisure and business travel halted. Public transit in the United States saw a dramatic reduction in usage, with some cities' transit ridership declining by as much as 90% (NYC MTA 2020). As it became clearer that the virus causing COVID-19 was transmitted via respiratory aerosols (Chia et al. 2020; Liu et al. 2020; Tang et al. 2020), transit agencies took measures to reduce the exposure to SARS-CoV-2 and the probability of infection for passengers and employees (APTA 2020; NYC MTA 2020). Initial reports asserted that public transit was a major vector for the transmission of SARS-CoV-2 (Harris 2020; Zhang et al. 2020), with others suggesting that the frequency of train services plays an important role in the spread of the pandemic (Hu et al. 2021).

Respiratory secretions can be aerosolized into virus-containing droplets or particles through daily activities, e.g., exhaling, talking, coughing, and sneezing (Chia et al. 2020). It is now generally accepted that there are two primary airborne modes of viral transmission for SARS-CoV-2: (a) larger droplets that travel short distances of the order of a few meters before settling by gravity; and (b) smaller airborne microdroplets ($<\sim 5$ μm) that are small enough to remain suspended in the air for longer periods and be inhaled. Hospital-based studies suggest that SARS-CoV-2 RNA in the air appears in distinct size ranges of 0.25–1.0 μm, 1.0–4.0 μm, and > 2.5 μm in aerodynamic diameter (Liu et al. 2020), with both the larger and smaller sizes contributing to the exposure.

Engineering controls, such as increased indoor ventilation, are recognized elements of the hierarchy of exposure controls for numerous hazards (NIOSH 2015a, 2015b), including infectious agents like SARS-CoV-2 (ASHRAE 2020a; CDC 2021; EPA 2021b). High-speed trains typically have high ventilation rates; however, increasing airflow through train car cabins may not always be feasible. Administrative controls, such as social-distancing measures, are not capable of reducing exposure to smaller particles. For example, a study carried out by Bazant and Bush (2021) indicated the inadequacy of the six-foot social distancing rule, further emphasizing the need for ventilation interventions. Several efforts have been carried out to document ventilation-related strategies to mitigate transmission of SARS-CoV-2-like aerosols in specific microenvironments — school buildings, healthcare settings, school buses, airplanes, and automobiles (Zitter et al. 2002; Anderson and Streifel 2007; Knibbs et al. 2009; Chaudhry and Elumalai 2020; Guthrie et al. 2020; NASEM 2020; Silcott et al. 2020; Mousavi et al. 2021).

While ventilation and filtration are integral parts of the air handling systems of train fleets, the COVID-19 public health crisis has focused increased attention on their performance. Mass-transit vehicles have heating, ventilation, and air conditioning (HVAC) systems that utilize a mixture of fresh and recirculated air, and it is important to assess the impact of the ratio of fresh to recirculated air in the cabin environment (Curtiss and Kreider 1992). While many public transit systems have minimum efficiency reported value MERV-8 filters as a default, upgrading these to MERV-13 filters would have the expected benefits. The use of high-efficiency particulate air (HEPA) room air purifiers has also been suggested as a possible additional safe-guard (Allen and Marr 2020; Lindsley et al. 2021; EPA 2021a). It is

important to assess the adequacy of these systems to provide safe and clean air to passengers and transit workers, and to prevent community spread of COVID-19 (ASHRAE 2020c; EPA 2021c).

In partnership with a large-scale, interstate, mass-transit rail company, a series of experiments was conducted in a fleet of stationary and moving passenger railcars to assess the adequacy of the train's HVAC systems to provide safe and clean air to passengers and transit employees, and to prevent community spread of COVID-19. The objectives were to determine the effects of several engineering controls on (1) the removal rate per hour of these aerosols; and (2) the estimated air changes per hour (ACH) in a fleet of passenger railcars under both static and dynamic conditions (i.e., when the train was stationary in the maintenance yard and moving, respectively), and to evaluate the effectiveness of the ventilation and air filtration systems in a range of representative conditions in reducing the probability of exposure. The engineering controls of interest included the:

1. the ratio of recirculated to fresh (i.e., outdoor) air (corresponding to two ventilation damper positions);

2. particle filtration efficiency of two different merv filters used in the hvac system; and

3. presence or absence of a portable hepa cabin air purifier system.

Methods

Heating, ventilation, and air conditioning (HVAC) system of railcar

Experimental investigations were carried out on flow rate in three railcars of the same fleet, representative of the rail company's most regularly used commuter passenger cars. Each railcar was 150.5 m^3 (5,314 ft^3) with a designed outdoor air intake flow rate of 34 m^3/min and a designed total supply air flow rate of 102 m^3/min. The air in the car is designed to be filtered 40.7 times per hour and replaced or changed with outdoor air 13.6 times per hour by the HVAC system. Outdoor air is brought into the railcars' return air duct (return plenum) through dampers that regulate the airflow. Here, the outdoor air mixes with the recirculated air, passes through a MERV-8 filter, then moves through the heating and cooling elements before entering the supply air duct (supply plenum) to be distributed back into the car volume. An exhaust blower removes a portion of the cabin air to the outside depending on the position of a ventilation damper. As designed, the fully open damper position corresponds to a ratio of 67:33 recirculated air (RA) to outdoor air (OA) and the closed damper position corresponds to 100% recirculation. However, given the age of the fleet, the RA:OA ratio when the damper is closed was closer to 90:10 due to air leakage from various openings in the cabins. The total flowrate through the car could not be changed. The railcars can operate at speeds up to 201 km/h (125 mph). Each cabin had 36 seats on each side of a central aisle, spread over 18 rows, overhead compartments above each row, and two bathrooms on one end (Figure 1).

The HEPA cabin air purifier system (OmniAire 600 V negative air machine, 150–550 cfm (4.2–15.4 m^3/min) clean air delivery rate (CADR), 8″ diameter exhaust collar, standard

HEPA and MERV-9 secondary filter) was chosen by the transit engineers and railcar operators based on its size, specifications, and ability to not compromise passenger comfort and seating. The HEPA air purifier unit was operated in the low and high fan conditions corresponding to 150 and 550 cfm nominal flow rates, respectively.

Generation of aerosol

Aerosols in the 0.3–5.0 μm size range were generated using a Collison nebulizer (MRE 3-jet with attached pressure gauge) with a 70:30 mixture of propylene glycol and vegetable glycerin. The nebulizer was placed in the center of the railcar between rows 10 and 11 (Figure 1), on a stand 1.0 m above the floor with the outlet 0.2 m above that for a total of 1.2 m. This height is equivalent to the distance from the floor to the middle part of the seat's headrest, making it a good approximation for the height of a person's breathing zone and the origin of particle dispersion.

The nebulizer was connected by an air supply line (3/8″; 200 psi; Continental ContiTech) to a high-pressure air supply (average pressure = 128.34 psi; standard deviation = 3.32 psi) located in the machine shop at the railyard (Figure S-1 in Supplementary Materials). A HEPA filter was placed in-line to filter the shop air before it entered the nebulizer. Each experimental run was carried out over a period of approximately 30 min, with the Collison nebulizer generating the aerosol for the first 15 min (aerosol concentration increase) and no aerosol generation for the second 15 min (aerosol concentration decrease). The intent was not to mimic human breathing or speaking but rather to observe the fate of aerosol particles of relevant sizes over time in the cabin.

Sampling instrumentation

Real-time aerosol concentrations were measured at four locations in the passenger cars using photodetector particle counters (AeroTrak Handheld Particle Counter – Model 9306; TSI; Shoreview, MN). Two instruments were placed on each side of the nebulizer, with one placed on a seat (0.5m from floor) and one elevated on the luggage rack (1.6m from floor) so that each half of the car had two AeroTraks representative of exposure at sitting and standing position respectively (Figure 1). The AeroTrak counts particles using a laser beam and a photodetector to detect light scattering and provides particle counts in six size ranges: 0.3–0.5μm, 0.5–1.0μm, 1.0–3.0μm, 3.0–5.0μm, 5.0–10.0μm, and >10.0μm. Each AeroTrak was calibrated daily, before beginning the experiments. Aerosol concentration measurements were logged at 1-min intervals for each experiment and downloaded to a computer as .csv files. Figure S-3 in the Supplementary Materials shows an example of a set of data from the four Aerotrak instruments for one particle size range (0.3–0.5μm) for one experimental condition.

Experimental design

Static conditions—The effects of the RA:OA ratio, the particle filtration efficiency of the HVAC filter, and the presence or absence of a portable HEPA cabin air purifier system on the removal rate per hour of the aerosol particles in different size ranges were studied under static conditions (i.e., when the train was stationary). The number of ACHs in the cars was

also measured under these effects with measurements repeated in three passenger cars of the same type.

The RA:OA ratio was determined by damper position (two positions 1 and 2, that nominally correspond to ratios of 90:10 and 67:33, respectively). The total air flowrate through the car could not be changed. The ventilation ACH delivered under each scenario of RA:OA fraction was estimated to be 13.4 ACH for 33% OA (close to the 13.6 ACH mentioned previously) and approximately 4.1 ACH for 10% OA. The portable HEPA unit was placed approximately 10.5 m away from the Collison nebulizer facing the direction of the test aerosol generation, as shown in Figure 1.

MERV-8 filters were used for the standard conditions according to standard operating procedures for the railcar HVAC system. These standard conditions were compared to those observed using a MERV-13 filter. MERV-8 filters maintain a particle removal efficiency that is negligible for 0.3–1.0 μm particles, >20% for 1.0–3.0 μm particles, and >70% for 3.0–10.0μm particles while MERV-13 filters' particle removal efficiencies are >50% for 0.3–1.0μm particles, >85% for 1.0–3.0 μm particles, and >90% for 3.0–10.0 μm particles (ASHRAE, 2020b). For both static and dynamic conditions, new filters were installed in each rail car prior to beginning experiments.

The experimental matrix for different ventilation scenarios is shown in Table 1. Standard operating conditions for this passenger car are reflected in experimental conditions 1 and 2. While the damper positions can be changed (i.e., changing the RA:OA ratio) under a variety of different circumstances (e.g., change in ambient temperature and traveling through urban vs rural areas), conversations with transit engineers and railcar operators indicated changing damper positions it is not typical practice. Similarly, while the use of MERV-8 filters is standard practice, the use of a MERV-13 filter and a cabin air purifier is not.

Dynamic conditions—During dynamic conditions, the experimental passenger car (without regular passengers, except for the study team) was moving as part of a train moving at an average speed between 117.5 and 136.8 km/h (73.0 and 85.0 mph), over approximately 480 km (298.3 miles). Given the constraints of a moving train, the ability to evaluate all combinations of the engineering controls was restricted. The recirculation ratio (damper position) and the HVAC filter type could not be changed; however, the HEPA air purifier unit could be turned on and off and operated in the low and high fan conditions and was included in the experimental matrix. The study design with the experimental conditions tested under dynamic conditions is shown in Table 2 and detailed experimental conditions are provided in the Supplementary Materials.

Calculating ACH values—The ventilation system design in the passenger cars is such that there is supply air coming in at regularly spaced intervals through a plenum along the sides of the car, while the return-air ducts are at both the ends of the car. A well-mixed room (WMR) model was applied to this situation. This models a room of volume (V, m^3) with a constant ventilation airflow rate of (Q, m^3/min) where an airborne particulate contaminant is being generated at some rate (G, the number of particles generated per unit time) to produce a contaminant concentration inside the room ($C(t)$, number of particles/m^3). At the end of the

15 min when the nebulizer is turned off and the contaminant generation ceases ($G = 0$), the concentration starts decreasing with time for the last 15-min of the experiment. This phase of the experiment is represented by the concentration decay equation for a WMR:

$$C(t) = C(0)exp\left(-\frac{Q + k_L V}{V}t\right),$$

(1)

where the exponential term $\left(\frac{Q + k_L V}{V}\right)$ is the total removal rate of the particles (in units of min^{-1}), including both ventilatory and non-ventilatory mechanisms. A regression of $In\left(\frac{C}{C(0)}\right)$ vs. $\left(\frac{Q + k_L V}{V}\right)$ was used to estimate ACH values in both static and dynamic conditions using data from the AeroTrak units that were placed at four different locations in the railcar. It should show roughly equivalent ACH values throughout the car if it is truly a WMR scenario. Any differences are likely due to spatial heterogeneity in ventilation patterns. This approach was also used to estimate the removal rate of larger particles (> 0.5 μm).

Estimating the probability of infection—A modeling approach following Miller et al. (2021) was used to estimate the probability of infection, assuming no one in the car is vaccinated. This standard approach was used to compare the risks of infection under the various intervention scenarios that we examined. Briefly, this approach assumes that all passengers maintain at least a 2 m (6 ft) distance between them. Because large droplets quickly settle out of the air, this social distancing limits the impact of larger droplets and focuses on probability due to smaller aerosol particles. The model makes the following major assumptions: (1) There is no prior infectious material in the car before the trip begins; (2) the latent period of the disease is longer than the length of the model; (3) infectious aerosols are evenly distributed throughout the cabin volume; and (4) infectious aerosols are removed by a first-order process that includes ventilation (air changes per hour or ACH), deposition, and viral inactivation.

In this model, the probability of infection is assumed to be related to the number of quanta (airborne virus) inhaled. Quanta (q) are used to represent infectious respiratory aerosol when the actual viral dose in the aerosol and the human dose response required to cause infection are unknown (Watanabe et al. 2010; Nishiura et al. 2020). The average concentration of quanta in a room (C_{avg}) can be estimated as:

$$C_{avg}(t) = \frac{G}{Q + k_L V}$$
$$\left(1 - \frac{1}{T\left(\frac{Q + k_L V}{V}\right)}\left(1 - exp\left(-\frac{Q + k_L V}{V}T\right)\right)\right)$$

(2)

Here, G is the quanta emission rate, $\left(\frac{Q + k_L V}{V}\right)$ is the sum of all loss processes (per hour), T is the duration of the trip in hours, and V is the volume of the cabin (cubic meters). The emission of quanta for SARS-CoV2 is an uncertain parameter and the estimated 50th percentile emissions for resting, speaking at light activity, and speaking loudly or singing

are 0.36, 4.9, and 31 q/hr, respectively (Curtiss and Kreider 1992). A value of 10 q/hr was assumed.

For all the modeling presented here, the deposition rate of virus-containing aerosols to surfaces was estimated as 0.3 hr^{-1}, assuming most particles are between 0.3 and 1.0 μm in a furnished room with low airspeed. Values between 0.1 and 10 hr^{-1} have been reported in the literature depending on airspeed and particle size distribution (Thatcher et al. 2002). The natural decay rate of the virus has been assumed to be 0.62 hr^{-1} (van Doremalen et al. 2020). By assuming a breathing rate of 0.8 m^3/hr for the passengers in the car, both the number of quanta inhaled by uninfected people and the probability of infection can be estimated. The probability infection (P_i) is modeled as

$$P_i = 1 - exp(-n),\qquad(3)$$

where n is the number of inhaled quanta (Sze To and Chao 2009). This can in turn can be modeled as $n = \frac{Ipqt}{Q}$, where I is the number of infectors, p is the pulmonary ventilation rate of a person, q is the quanta generation rate, t is the exposure time interval, and Q is the room ventilation rate with clean air. The quanta required for an infection to occur remains a highly uncertain value for SARS-CoV-2 (Miller et al. 2021). The expected number of cases can be obtained by multiplying the probability of infection by the number of uninfected people in the railcar.

Statistical analysis

An analysis of variance (ANOVA) was run for both static and dynamic conditions to examine the effect of damper position, filter type, and use of a portable air purifier on the average particle removal rates (hr^{-1}) across all five cut sizes for each condition. Post-hoc pairwise comparisons of means were conducted to identify which exposure-control measures were responsible for differences seen in removal rate across particle sizes for each condition.

Additionally, multilevel mixed-effects linear regression models with random intercepts determined whether significant differences in removal rate between engineering control types used in both static and dynamic conditions existed. For static conditions, the damper position was coded as 1=position 1 for a RA:OA ratio of 90:10, 0=position 2 for a RA:OA ratio of 67:33; filter type was coded as 1=MERV-13, 0=MERV-8; and air purifier use was coded as 1=yes, 0=no. For dynamic conditions, air purifier use was coded as 1=fan used and 0=fan not used. The impact of engineering control types (damper, filter, air purifier) on removal rate was assessed, focusing on all control types for the static model and the use of the air purifier alone for the dynamic impacted removal rates. STATA (Version 15.1, StataCorp, College Station, TX) was used for the analysis.

Results

Size distribution generated by collison nebulizer

The particle sizes of the droplets generated by the Collison nebulizer were experimentally determined to be lognormally distributed as shown in Figure 2, with a geometric mean

diameter of 0.19μm and a geometric standard deviation of 1.55. The number concentration (#/m^3) of aerosols generated during different ventilation conditions are provided in the Supplementary Materials (Figures S-4–S-6).

Effect of ventilation parameters on particle removal rates

Static conditions—Figure 3 shows the effect of damper position, filter type, and presence or absence of a HEPA air purifier on the average removal rates of particles in different size ranges. Average particle removal rates were obtained from the measurements collected from three runs each at four locations for three cars by the AeroTrak for each experimental condition. The median removal rates increase with particle size for each condition.

An analysis of between- and within-experimental condition variability showed that mean removal rate (± standard deviation, coefficient of determination) values ranged from a low of 8.79hr^{-1} (± 3.89hr^{-1}, R^2 =0.95) for particles 0.3–0.5mm to a high of 12.86hr^{-1} (± 8.29hr^{-1}, R^2 = 0.75) for particles 5.0–10.0μm (Table S-1, Supplementary Materials). Table 3 shows that across various particle size ranges, mean removal rate values were on average highest in Condition 7 (damper position corresponding to RA:OA ratio of 90:10, MERV-13, HEPA air purifier on high) and lowest in Condition 3 (damper position corresponding to RA:OA ratio of 90:10, MERV-8, HEPA air purifier on high). Table 4 shows that mean removal rate values were highest with the use of MERV-13 filters and lowest, on average, with a MERV-8.

ANOVA and post-hoc significance tests revealed that only MERV-13 filters significantly impacted removal rates for all particle size ranges ($p < 0.01$) while recirculation ratios were marginally significant ($p < 0.1$) only for the largest size range (Table 5). The use of the portable HEPA air purifier did not significantly affect removal rates.

A mixed-effects linear regression model was used to determine significant differences in ACH between the conditions based on engineering control type (recirculation ratio, MERV filter rating, presence of air purifier) for each size range. Standard errors for each fixed-effect covariate (engineering control type) and the residual variance from the random-effects intercepts were calculated for each particle size. The results of this model are summarized in Table 6. Equation 4 can be used to estimate the particle removal rates for different conditions, where RA:OA ratio = 1 for 90:10 and 0 for 67:33, MERV filter rating =1 for MERV-13 and 0 for MERV-8, and Air Purifier =1 if present and 0 if absent.

$$
\begin{aligned}
&Aerosol\ Removal\ Rate\big(hr^{-1}\big) \\
&= 7.03 + (0.34 \times Recirc.\ Ratio) \\
&+ (6.46 \times MERV\ Rating) \\
&+ (0.08 \times Air\ Purifier\ Presence)
\end{aligned}
\tag{4}
$$

Using particles 0.3–0.5 μm as an example, the average removal rate is 7.03 hr^{-1} when the RA:OA ratio is 67:33, a MERV-8 filter is used, and no air purifier is present. Using a MERV-13 filter compared to a MERV-8 filter improved the removal rate across all particle sizes (Figure 4). The results of the regression are consistent with the ANOVA and show that

regardless of particle size when controlling for the effects of each condition, only filter type significantly impacted the removal rate.

Dynamic conditions—Between- and within-experimental condition variability showed that mean removal rate (± standard deviation, coefficient of determination) values ranged from 9.04 hr^{-1} (± 1.14 hr^{-1}, $R^2 = 0.99$) for particles 0.3–0.5 μm to 17.56 hr^{-1} (± 6.08 hr^{-1}, $R^2 = 0.83$) for particles 5.0–10.0 μm (Table S-1, Supplementary Materials). Figure 5 shows that mean removal rate values were on average highest while the train was in motion but without the use of the HEPA air purifier.

For particles less than 1.0 μm, mean removal rate values were on average highest when the HEPA air purifier was off. For particles greater than 1.0 μm, mean removal rates were highest when the HEPA air purifier was set to high speed (Tables 3 and 4).

As the recirculation ratio and filter MERV rating could not be changed during dynamic conditions, an ANOVA was run to examine only the effects of the use of a portable HEPA air purifier on particle removal rates across all five size ranges. The use of the HEPA air purifier at both low and high fan speeds (150 and 550 cfm, i.e., 4.2 and 15.4m^3/min, CADR, respectively) showed a statistically significant difference in the removal rate of aerosols 1.0 μm when compared to not using the air purifier ($p < 0.05$), particularly when comparing removal rates at the low fan setting to those seen without the use of the air purifier (Table 5).

A mixed-effects linear regression model determined whether significant differences in removal rate existed when the air purifier was turned off and on at different fan speeds (Table 6). Standard errors for each fixed-effect covariate (engineering control type) and the residual variance from the random-effects intercepts were calculated for each particle size. Equation 5 can be used to estimate the particle removal rates when using a HEPA air purifier at different settings, with Air Purifier Presence, High =1 and Air Purifier Presence, Low =0 if the fan was on high speed and the reverse if the fan was on low speed. No variables were present for the recirculation ratio or the filter rating as those controls remained constant during dynamic testing (RA:OAthe = 90:10 and MERV8 filter, respectively). As an example, for particles 0.3–0.5μm, the average removal rate with a RA:OA = 90:10, a MERV-8 filter, and the air purifier on high fan speed was 9.13hr^{-1}. Under the same conditions but with the air purifier on low fan speed, the average removal rate for particles 0.3–0.5μm was 7.73hr^{-1}. Results for other particle sizes can be found in Table 6.

$$\begin{aligned} Aerosol\ Removal\ Rate(hr^{-1}) \\ = 10.26 - (2.53 \times Air\ Purifier\ Presence,\ Low) \\ -(1.13 \times Air\ Purifier\ Presence,\ High) \end{aligned} \quad (5)$$

Modeled probability of exposure to infectious aerosols

Figure 6 shows the distribution of infection probability after exposure to infectious aerosols in a railcar under normal operating conditions (with a MERV-8 filter only), when the filter is upgraded to a MERV-13, when a HEPA air purifier is present in the cabin (with MERV-8

filter), and when there is a MERV-13 filter and a HEPA air purifier in the cabin. The median probability of exposure is 6 per 10,000 under standard conditions and the risk is unchanged with the introduction of a HEPA air purifier. The probability of exposure is reduced to 3.5 per 10,000 with the MERV-13, and further to 3 per 10,000 when there is a MERV-13 filter and a HEPA air purifier.

Discussion

Key findings

This study presents experimental results on the removal rates of particles in the size ranges of SARS-CoV-2 viral aerosols from stationary and moving passenger railcars, and the air changes per hour provided by the existing and modified air handling systems. The effect of ventilation and air filtration (HVAC) systems on removal rates and their effects on estimated probability of infection was evaluated in a range of representative conditions: (1) under different ratios of recirculated to fresh (i.e., outdoor) air; (2) using MERV filters with standard (MERV-8) and increased (MERV-13) filtration ratings; and (3) in the presence and absence of a HEPA room air purifier system. The study developed methods for generating aerosols in the size ranges of SARS-CoV-2 viral aerosols reported in the literature. To the authors' knowledge, this is one of the first studies of this kind in public transit systems, especially for long-distance commuting, where passengers are likely to spend significant amounts of time.

Since the study team did not have direct access to the ventilation ducts and the HVAC system, the air changes per hour (ACH) values were estimated using the removal rates of the smallest particle sizes (<0.5μm) from the railcars. The estimated ACH values were lower than the reported design ACH values, not surprising given the aging railcars in this fleet. The results indicate that the median removal rates increase with particle size for each experimental condition. The smallest particle sizes get removed primarily by ventilation, and in fact, their removal rates can be used as a good approximation for the ACH. As particle size increases, other mechanisms such as gravitational settling play an increasingly important role.

Increasing the efficiency of the HVAC filters in the railcar (i.e., upgrading from MERV-8 to MERV-13 rated filters) increased the removal rate of the smallest particles from the space, and reduced the probability of infection to SARS-CoV-2 viral particles. While this was the only variable that had a statistically significant effect on aerosol removal rate, increasing filter efficiency comes at the cost of increased operating expenditures (energy expenditure to overcome increased pressure drop across a more efficient filter) and capital costs for system upgrades (replacing lower cost MERV-8 with higher cost MERV-13 filters).

The ratio of recirculated to outdoor air has a minimal effect on the removal rates of particles of different sizes, although we could test only two ratios in this study.

Study limitations

We found that placing a HEPA air purifier in the railcar cabin did not make a significant difference to particle removal rates across the four locations where these were measured.

However, this could be due to several things. First, the selection and placement of the air purifier in the railcar were done with passenger seating availability and comfort in mind. That is, the unit was placed in an open luggage-storage area where it would not take up passenger seating, including spaces reserved for passengers with mobility issues, nor where noise levels from the fan would have exceeded 85 dBA (the NIOSH Recommended Exposure Limit for occupational noise exposure). As a result, the CADR of the air purifier selected was 15.4m^3/min (550 cfm), considerably less than the total airflow through the cabin of 102m^3/min. At the same time, this might not have been the optimum location from a ventilation perspective, and the air cleaner location did not permit a full evaluation of its potential role in particle removal. A reasonably thorough study of this topic would involve several units located throughout the railcar tested under different operational conditions. Second, the lack of particle removal seen with the air purifier could also speak to the effectiveness of the HVAC's air filters. New filters were installed in each rail car before testing under both static and dynamic conditions. The effectiveness of MERV filters in HVAC systems is well documented (McCarthy et al. 2013; Fisk and Chan 2017; Schoen 2020; EPA 2021c). Therefore, it is likely that particle removal rates did not change greatly in the presence of the air purifier because the particles had already been effectively removed by the MERV filters. Despite this, the HEPA air purifier showed a slight effect on the average particle removal rate during dynamic testing, particularly for particles smaller than 1mm, with removal rates increasing with the use of the air purifier on the highest *vs.* lowest fan speed setting. This may be due to additional airflow through the cabin as the train was in motion at speeds exceeding 100km/h (see Table 2).

Although this work is a key step in assessing the effectiveness of various exposure control methods to SARS-CoV-2 aerosols, it is limited in that some of the experimental conditions (the filter type and air recirculation ratio) could not be evaluated during dynamic testing. Additionally, confirmation of the air purifier's effectiveness could not be fully determined as no experiments were run using it alone as a source of exposure control. Furthermore, no measurements were taken with passengers in the cabin, limiting the evaluation of human behavior on aerosol transport. However, as the same railcar was used in both the static and dynamic tests, and as similar HVAC systems are used in both the railcars and the types of locomotives evaluated, it is reasonable to consider that similar results would be seen when the railcar is in motion. Other potential interventions such as the use of germicidal ultraviolet light in HVAC systems (Reed 2010; Biasin et al. 2021), nanosilver-coated filters (Joe et al. 2016), or germicidal vapors and aerosols (Puck 1947) were not able to be investigated in this study.

Finally, the probability calculation adopted the approach of Miller et al. (2021) that used the Skagit Valley Outbreak to model the probability of infection which used the Wells-Riley model of infection and the actual cases of COVID resulting from one infected person to calculate the probability of infection to infer the number of quanta required to cause infection. The median probability of exposure is 6 per 10,000 under standard conditions and the probability is unchanged with the introduction of a HEPA air purifier. The probability of exposure is reduced to 3.5 per 10,000 with the MERV-13, and further to 3 per 10,000 when there is a MERV-13 filter and a HEPA air purifier. Thus, there is a 41% reduction in the probability of exposure when the filter is upgraded to a MERV-13 and a 50%

reduction in the probability of exposure when the filter is upgraded to a MERV-13 and a HEPA air purifier is used in the cabin. This model assumed an unvaccinated population and was developed before the advent of the vaccines and recent Delta and Omicron coronavirus variants — factors that will affect the probability of infection. Further research should examine how more transmissible variants and the impact widespread vaccination and immunity might have on the effectiveness of these controls.

These findings are consistent with previous studies that showed the low probability of exposure to SARS-CoV-2 from the use of mass transit systems when the route of exposure is via aerosol inhalation, including aircraft (Silcott et al. 2020), high-speed trains (Zhang et al. 2020), urban buses (Zhang et al. 2021), and cars, buses, and autorickshaws (Das and Ramachandran 2021).

Conclusions

The results presented here show that a simple upgrade of the efficiency of the HVAC filters from MERV-8 to MERV-13 in public transit vehicles results in a clear reduction in the probability of infection. Other interventions studied such as the ratio of outdoor to recirculated air and the use of HEPA air purifiers did not have a significant effect on the probability of infection. Widespread upgrading of HVAC filter efficiency in public transit vehicles could help reduce the extent of community-spread infectious respiratory diseases. The benefits of such upgrades need to be balanced against the cost of increased operating expenditures and capital costs. Further studies are required on the effects of other potential interventions.

Supplementary Material

Refer to Web version on PubMed Central for supplementary material.

Acknowledgments

Data availability

The data underlying this article will be shared on reasonable request consistent with protections for the privacy of study participants and existing multi-party agreements.

References

Allen JG, Marr LC. 2020. Recognizing and controlling airborne transmission of SARS-CoV-2 in indoor environments. Indoor Air. 30(4):557–558. doi:10.1111/ina.12697. [PubMed: 32557915]

American Public Transportation Association (APTA). 2020. The COVID-19 pandemic. Public transportation responds: safeguarding riders and employees.

American Society of Heating, Refrigerating and Air-Conditioning Engineers (ASHRAE). 2020a. ASHRAE resources available to address COVID-19 concerns. In: Simmons S, editor. Atlanta (GA): ASHRAE.

American Society of Heating, Refrigerating and Air-Conditioning Engineers (ASHRAE). 2020b. Filtration and air cleaning summary; [accessed 2022 Feb 18]. https://www.ashrae.org/technical-resources/filtration-disinfection.

American Society of Heating, Refrigerating and Air-Conditioning Engineers (ASHRAE). 2020c. In-room air cleaner guidance for reducing Covid-19 in air in your space/room. Online: ASHRAE; [updated January 21, 2020; accessed 2022 Feb 18]. https://www.ashrae.org/technical-resources/filtration-disinfection.

Anderson JG, Streifel A. 2007. Airborne infectious disease management: methods for temporary negative pressure isolation. St. Paul (MN): Minnesota Department of Health.

Bazant MZ, Bush JWM. 2021. A guideline to limit indoor airborne transmission of COVID-19. Proc Natl Acad Sci USA. 118(17):e2018995118. doi:10.1073/pnas.2018995118.

Biasin M, Bianco A, Pareschi G, Cavalleri A, Cavatorta C, Fenizia C, Galli P, Lessio L, Lualdi M, Tombetti E, et al. 2021. UV-C irradiation is highly effective in inactivating SARS-CoV-2 replication. Sci Rep. 11(1):6260. doi:10.1038/s41598-021-85425-w.[PMC][33737536. [PubMed: 33737536]

Chaudhry SK, Elumalai SP. 2020. The influence of school bus ventilation scenarios over in-cabin PM number concentration and air exchange rates. Atmos Pollut Res. 11(8):1396–1407.

Chia PY, Coleman KK, Tan YK, Ong SWX, Gum M, Lau SK, Lim XF, Lim AS, Sutjipto S, Lee PH, et al. 2020. Detection of air and surface contamination by SARS-CoV-2 in hospital rooms of infected patients. Nat Commun. 11(1):2800. [PubMed: 32472043]

Curtiss PK, Kreider JF. 1992. Laboratory tests of the nonlinearity of outdoor air percentage as a function of damper position and induced inlet pressure. ASHRAE Trans. 98: 196–202.

Das D, Ramachandran G. 2021. Risk analysis of different transport vehicles in India during COVID-19 pandemic. Environ Res. 199:111268. [PubMed: 33984308]

Fisk WJ, Chan WR. 2017. Effectiveness and cost of reducing particle-related mortality with particle filtration. Indoor Air. 27(5):909–920. doi:10.1111/ina.12371. [PubMed: 28170103]

Guthrie BL, Tordoff DM, Meisner J, Tolentino L, Jiang W, Fuller S, Green D, Louden D, Ross JM. 2020. Summary of school re-opening models and implementation approaches during the COVID-19 pandemic online. Washington State Department of Health; University of Washington Metacenter; Start Center.

Harris JE. 2020. The subways seeded the massive coronavirus epidemic in New York City. SSRN Electron J. doi:10.2139/ssrn.3574455.

Hu M, Lin H, Wang J, Xu C, Tatem AJ, Meng B, Zhang X, Liu Y, Wang P, Wu G, et al. 2021. Risk of coronavirus disease 2019 transmission in train passengers: an epidemiological and modeling study. Clin Infect Dis. 72(4):604–610. [PubMed: 32726405]

Joe YH, Park DH, Hwang J. 2016. Evaluation of Ag nanoparticle coated air filter against aerosolized virus: antiviral efficiency with dust loading. J Hazard Mater. 301: 547–553. doi: 10.1016/j.jhazmat.2015.09.017. [PubMed: 26434534]

Knibbs LD, de Dear RJ, Atkinson SE. 2009. Field study of air change and flow rate in six automobiles. Indoor Air. 19(4):303–313. [PubMed: 19500174]

Lindsley WG, Derk RC, Coyle JP, Martin SB Jr, Mead KR, Blachere FM, Beezhold DH, Brooks JT, Boots T, Noti JD. 2021. Efficacy of portable air cleaners and masking for reducing indoor exposure to simulated exhaled SARS-CoV-2 aerosols. MMWR Morb Mortal Wkly Rep. 70(27):972–976. [PubMed: 34237047]

Liu Y, Ning Z, Chen Y, Guo M, Liu Y, Gali NK, Sun L, Duan Y, Cai J, Westerdahl D, et al. 2020. Aerodynamic analysis of SARS-CoV-2 in two Wuhan hospitals. Nature. 582(7813):557–560. [PubMed: 32340022]

McCarthy MC, Ludwig JF, Brown SG, Vaughn DL, Roberts PT. 2013. Filtration effectiveness of HVAC systems at near-roadway schools. Indoor Air. 23(3):196–207. doi:10.1111/ina.12015. [PubMed: 23167831]

Miller SL, Nazaroff WW, Jimenez JL, Boerstra A, Buonanno G, Dancer SJ, Kurnitski J, Marr LC, Morawska L, Noakes C. 2021. Transmission of SARS-CoV-2 by inhalation of respiratory aerosol in the Skagit Valley Chorale super-spreading event. Indoor Air. 31(2):314–323. [PubMed: 32979298]

Mousavi ES, Kananizadeh N, Martinello RA, Sherman JD. 2021. COVID-19 outbreak and hospital air quality: a systematic review of evidence on air filtration and recirculation. Environ Sci Technol. 55(7):4134–4147. doi:10.1021/acs.est.0c03247. [PubMed: 32845618]

National Academies of Sciences Engineering Medicine (NASEM). 2020. Reopening K-12 schools during the COVID-19 pandemic: prioritizing health, equity, and communities. Washington (DC): The National Academies Press.

National Institute for Occupational Safety and Health (NIOSH). 2015a. Directory of engineering controls. Online: NIOSH; [updated January 14, 2015; accessed 2021 Jul 20]. https://www.cdc.gov/niosh/engcontrols/default.html.

National Institute for Occupational Safety and Health (NIOSH). 2015b. Hierarchy of controls. Online: NIOSH; [updated January 13, 2015; accessed 2021 Jul 22]. https://www.cdc.gov/niosh/topics/hierarchy/default.html.

New York City Metropolitan Transportation Authority (NYC MTA). 2020. Subway and bus ridership for 2020. MTA; [accessed 2021 Jun 11]. https://new.mta.info/agency/new-york-city-transit/subway-bus-ridership-2020.

Nishiura H, Oshitani H, Kobayashi T, Saito T, Sunagawa T, Matsui T, Wakita T, Suzuki M. 2020. Closed environments facilitate secondary transmission of coronavirus disease 2019 (COVID-19). medRxiv.

Puck TT. 1947. The mechanism of aerial disinfection by glycols and other chemical agents: I. Demonstration that the germicidal action occurs through the agency of the vapor phase. J Exp Med. 85(6):729–739. doi:10.1084/Jem.85.6.729. [PubMed: 19871646]

Reed NG. 2010. The history of ultraviolet germicidal irradiation for air disinfection. Public Health Rep. 125(1): 15–27. doi: 10.1177/003335491012500105.

Schoen L. 2020. Guidance for building operations during the COVID-19 pandemic. ASHRAE J. 72–74. https://www.ashrae.org/file%20library/technical%20resources/ashrae%20journal/2020journaldocuments/72-74_ieq_schoen.pdf.

Silcott D, Kinahan S, Santarpia J, Silcott B, Silcott R, Silcott P, Silcott B, Distelhorst S, Herrera V, Rivera D, et al. 2020. TRANSCOM/AMC commercial aircraft cabin aerosol dispersion tests. Technical report for the United States Transportation Command (USTRANSCOM) of the US Department of Defense and the Air Mobility Command of the US Air Force. https://apps.dtic.mil/sti/citations/AD1117734.

Sze To GN, Chao CY. 2010. Review and comparison between the Wells-Riley and dose-response approaches to risk assessment of infectious respiratory diseases. Indoor Air. 20(1):2–16. doi: 10.1111/j.1600-0668.2009.00621.x. [PubMed: 19874402]

Tang S, Mao Y, Jones RM, Tan Q, Ji JS, Li N, Shen J, Lv Y, Pan L, Ding P, et al. 2020. Aerosol transmission of SARS-CoV-2? Evidence, prevention and control. Environ Int. 144:106039.

Thatcher TL, Lai ACK, Moreno-Jackson R, Sextro RG, Nazaroff WW. 2002. Effects of room furnishings and air speed on particle deposition rates indoors. Atmos Environ. 36(11):1811–1819.

U.S. Centers for Disease Control and Prevention (CDC). 2021. Ventilation in buildings. Online: CDC; [updated June 2, 2021; accessed 2021 Jul 22]. https://www.cdc.gov/coronavirus/2019-ncov/community/ventilation.html.

U.S. Environmental Protection Agency (EPA). 2021a. Air cleaners, HVAC filters, and coronavirus (COVID-19). Online: EPA; [updated January 4, 2022; accessed 2022 Feb 18]. https://www.epa.gov/coronavirus/air-cleaners-hvac-filters-and-coronavirus-covid-19.

U.S. Environmental Protection Agency (EPA). 2021b. Ventilation and Coronavirus (COVID-19). Online: EPA; [updated January 4, 2022; accessed 2022 Feb 18]. https://www.epa.gov/coronavirus/ventilation-and-coronavirus-covid-19.

U.S. Environmental Protection Agency (EPA). 2021c. What is a MERV rating? Online: EPA; [updated March 3, 2021; accessed 2021 Jul 21]. https://www.epa.gov/indoor-air-quality-iaq/what-merv-rating-1.

van Doremalen N, Bushmaker T, Morris DH, Holbrook MG, Gamble A, Williamson BN, Tamin A, Harcourt JL, Thornburg NJ, Gerber SI, et al. 2020. Aerosol and surface stability of SARS-CoV-2 as compared with SARS-CoV-1. N Engl J Med. 382(16):1564–1567. doi:10.1056/NEJMc2004973. [PubMed: 32182409]

Watanabe T, Bartrand TA, Weir MH, Omura T, Haas CN. 2010. Development of a dose-response model for SARS coronavirus. Risk Anal. 30(7):1129–1138. doi:10.1111/j.1539-6924.2010.01427.x. [PubMed: 20497390]

World Health Organization (WHO). 2021. Naming the coronavirus disease (COVID-19) and the virus that causes it. Online: WHO; [accessed 2021 Jul 20]. https://www.who.int/emergencies/diseases/novel-coronavirus-2019/technical-guidance/naming-the-coronavirus-disease-(covid-2019)-and-thevirus-that-causes-it.

Zhang Y, Zhang A, Wang J. 2020. Exploring the roles of high-speed train, air and coach services in the spread of COVID-19 in China. Transp Policy (Oxf). 94:34–42. [PubMed: 32501380]

Zhang Z, Han T, Yoo KH, Capecelatro J, Boehman AL, Maki K. 2021. Disease transmission through expiratory aerosols on an urban bus. Phys Fluids. 33(1):015116.

Zitter JN, Mazonson PD, Miller DP, Hulley SB, Balmes JR. 2002. Aircraft cabin air recirculation and symptoms of the common cold. JAMA. 288(4):483–486. [PubMed: 12132979]
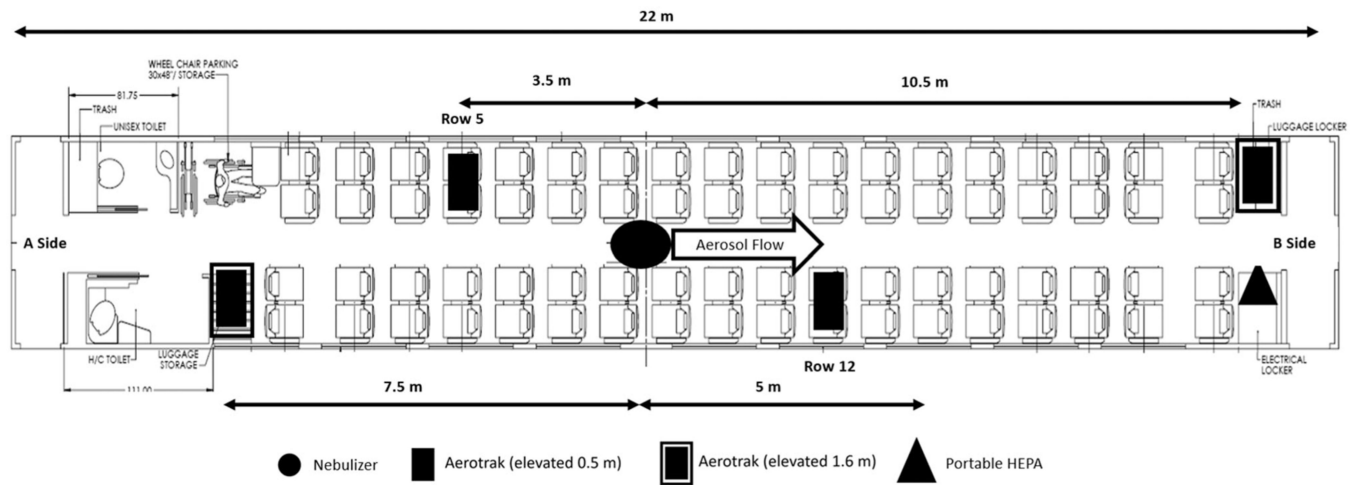
Figure 1.
Schematic of passenger car, drawn to scale with distances in meters.
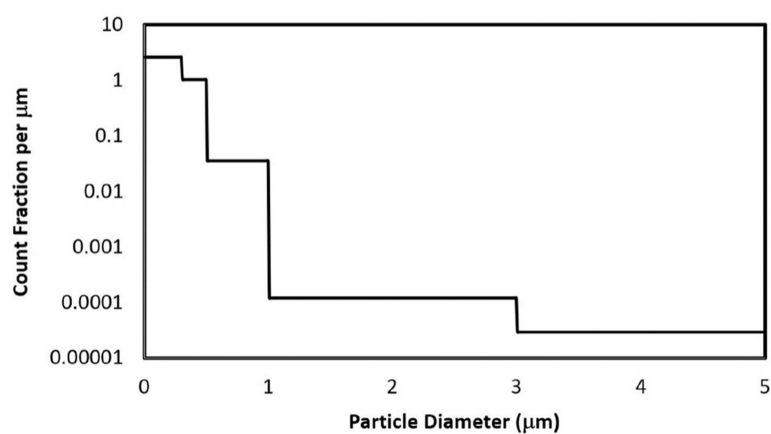
Figure 2.
Histogram of count fraction per micrometer *vs.* particle diameter.
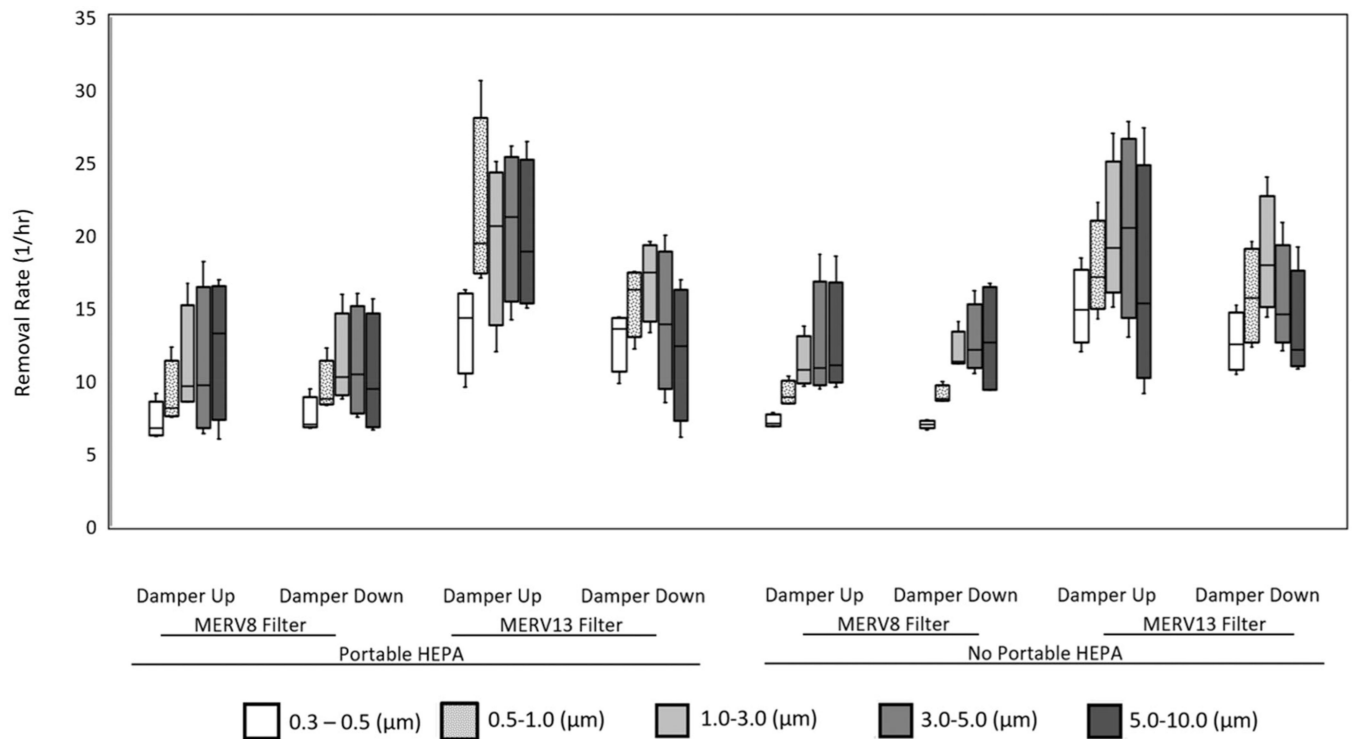
Figure 3.
Comparison of aerosol removal rates per hour across different experimental conditions during static testing in passenger railcars. Note that "Damper Up" refers to the open damper position (67:33 RA:OA) and "Damper Down" refers to the closed damper position (90:10 RA:OA).
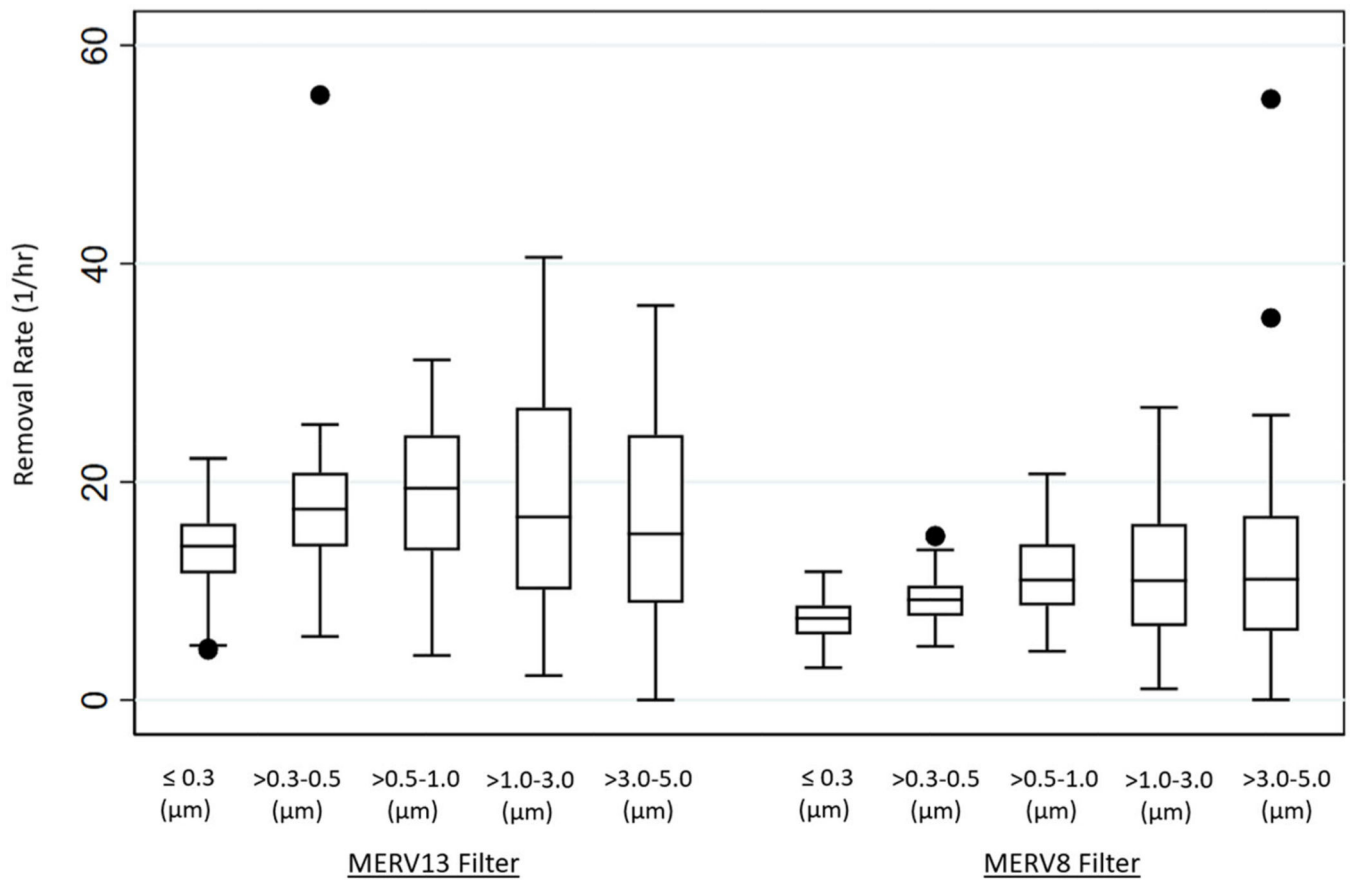
Figure 4.
Aerosol removal rates during static testing across all particle sizes using MERV13 and
MERV8 filters.
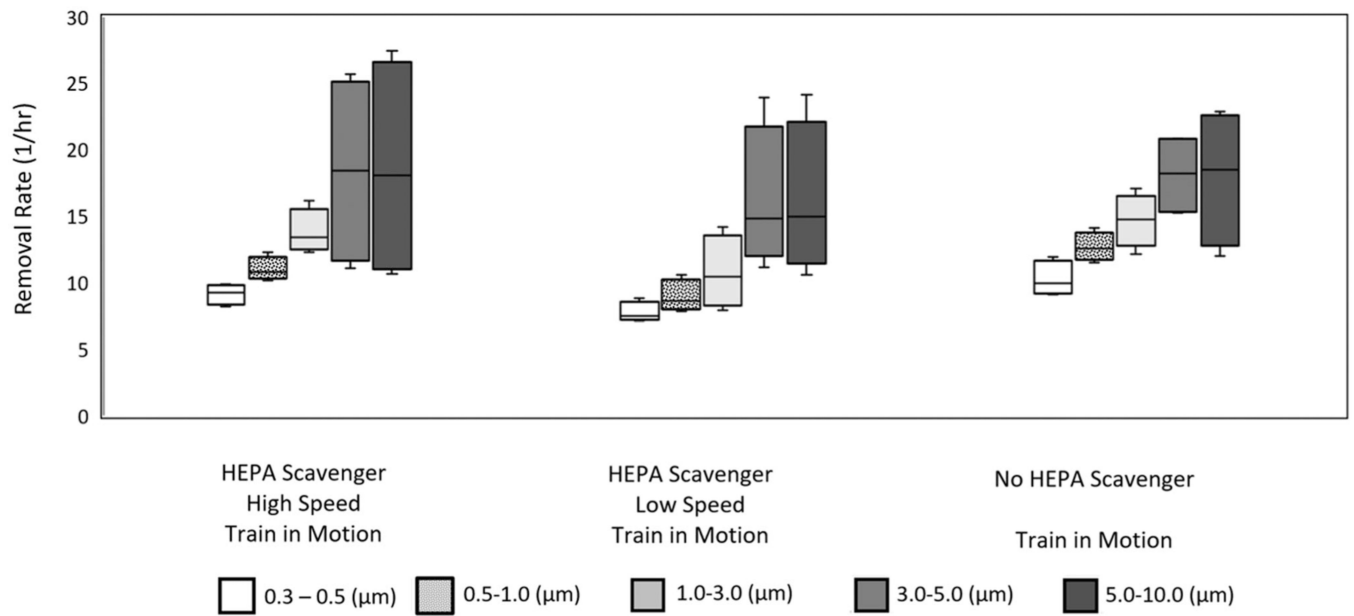
Figure 5.
Comparison of aerosol removal rates per hour for smaller particles (0.3–0.5 μm, and 0.5–1.0 μm) and larger particles (1.0–3.0 μm, 3.0–5.0 μm, and 5.0–10.0 μm) across different experimental conditions during dynamic testing in passenger railcars.
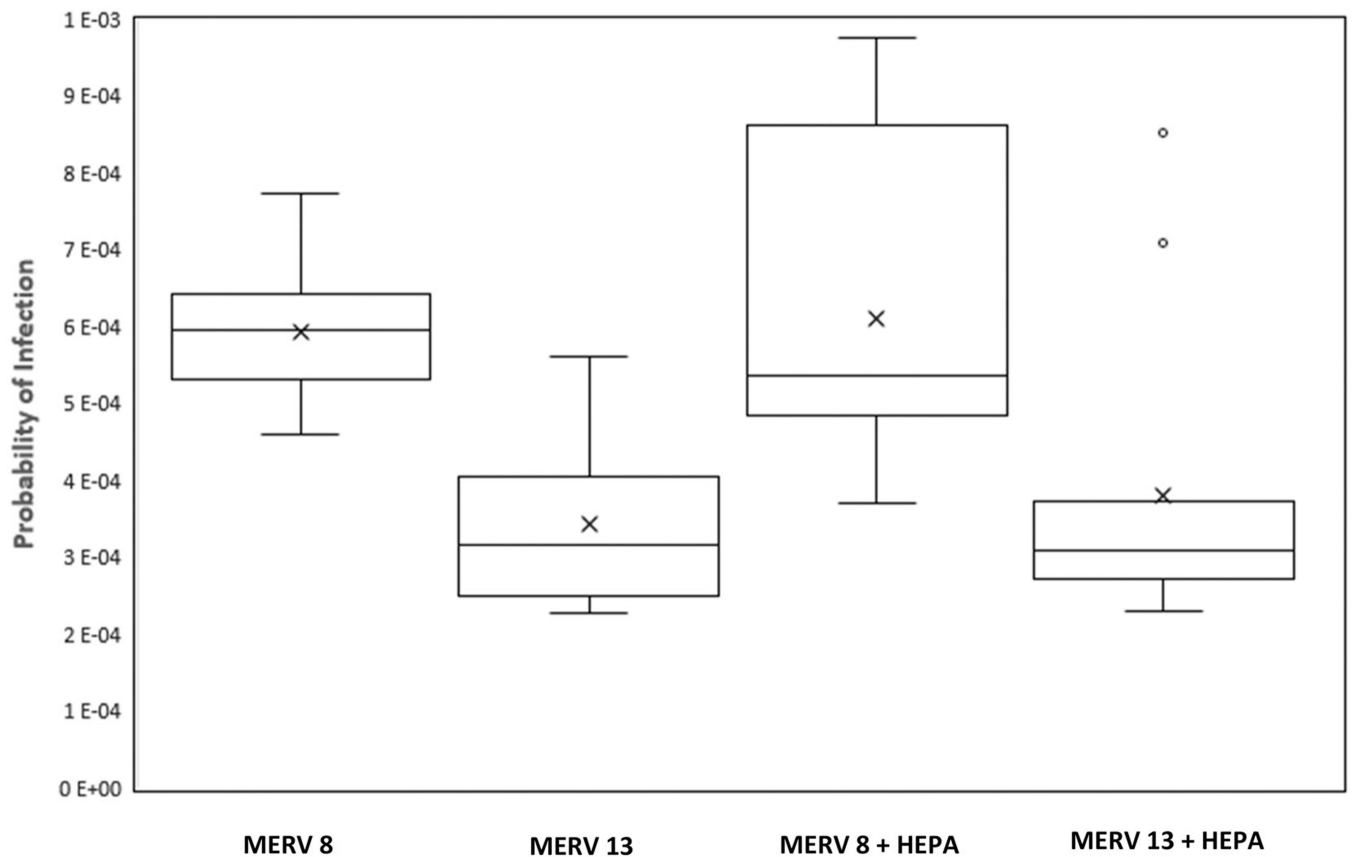
Figure 6.
Distribution of infection probability after exposure to infectious aerosols in a railcar under the conditions of: (a) standard conditions with a MERV-8 filter; (b) filter upgraded to a MERV-13 (c) with a MERV-8 filter and a HEPA air purifier in the cabin; and (d) filter upgraded to a MERV-13 and a HEPA air purifier in the cabin.

Table 1.

Study design showing the eight experimental conditions tested in each of the three railcars under static conditions.

Experimental condition	Recirculation ratio [a] (Physical Position)	Filter type [b]	HEPA scavenger (Fan Speed)	Number of experimental runs (in each car)
1	90:10 (Position 1 Up)	MERV 8	Absent	3
2	67:33 (Position 2 Down)	MERV 8	Absent	3
3	90:10 (Position 1 Up)	MERV 8	Present (High)	3
4	67:33 (Position 2 Down)	MERV 8	Present (High)	3
5	90:10 (Position 1 Up)	MERV 13	Absent	1 [c]
6	67:33 (Position 2 Down)	MERV 13	Absent	1 [c]
7	90:10 (Position 1 Up)	MERV 13	Present (High)	1 [c]
8	67:33 (Position 2 Down)	MERV 13	Present (High)	1 [c]

[a] Ratio of fresh (i.e., outdoor) to recirculated air; damper positions identified by train staff with numbers 1 and 2 corresponding to ratios of 90:10 and 67:33, respectively.

[b] New filters were installed in each rail car prior to testing.

[c] Only one run for this scenario since MERV13 filters are not standard on cars in operation and for concern of HVAC overload.

Table 2.

Study design showing the five experimental conditions tested in railcars under dynamic conditions.

Experimental condition [a]	Recirculation ratio [a,b] (*Physical Position*)	Filter type [a,b]	HEPA scavenger (*Fan speed*)	Average moving speed (km/h)	Number of experimental runs
1	90:10 (*Position 1 Up*)	MERV 8	Present (*High*)	132	3
2	90:10 (*Position 1 Up*)	MERV 8	Present (*Low*)	135	3
5	90:10 (*Position 1 Up*)	MERV 8	Absent	118	3

[a] Experimental conditions 3 and 4 occurred during a layover and were not included in the analysis as the railcars were not moving.

[b] A new filter was installed prior to departure. This was not able to be changed while the train was in motion.

[c] Ratio of fresh (i.e., outdoor) to recirculated air; damper positions identified by train staff with numbers 1 and 2 corresponding to ratios of 90:10 and 67:33, respectively.

[d] Average moving speed = distance traveled/total time in motion

Table 3.

Average particle removal rate (hr^{-1}) by condition under static and dynamic conditions.

Condition No.	No. of Observations	0.3–0.5 μm* Mean (SD)	0.5–1.0μm Mean (SD)	1.0–3.0μm Mean (SD)	3.0–5.0μm Mean (SD)	5.0–10.0μm Mean (SD)
Removal rate (hr^{-1})	under static conditions					
1	36	7.21 (1.20)	9.13 (1.46)	11.21 (3.39)	12.47 (7.21)	12.57 (7.25)
2	40	7.06 (1.22)	9.04 (1.53)	11.86 (2.82)	12.47 (6.17)	12.53 (7.66)
3	36	7.20 (2.30)	8.76 (2.62)	11.12 (3.91)	10.97 (5.54)	12.35 (9.57)
4	34	7.52 (2.73)	9.51 (2.97)	11.54 (3.62)	11.30 (4.89)	10.23 (5.82)
5	12	15.05 (4.86)	17.70 (5.24)	20.07 (7.48)	20.47 (11.47)	16.78 (10.99)
6	12	12.65 (4.05)	15.79 (4.98)	18.56 (6.00)	15.51 (8.75)	13.57 (8.26)
7	11	13.96 (5.44)	20.80 (13.02)	20.28 (8.80)	21.27 (11.63)	20.11 (10.73)
8	11	13.11 (3.42)	15.85 (3.47)	17.27 (4.49)	14.56 (6.46)	12.46 (6.45)
Removal rate (hr^{-1}) under dynamic conditions						
1	4	9.13 (0.83)	11.02 (0.91)	13.80 (1.68)	18.41 (7.29)	18.54 (8.42)
2		7.73 (0.75)	8.92 (1.23)	10.77 (2.76)	16.17 (5.44)	16.17 (5.77)
5		10.26 (1.32)	12.70 (1.09)	14.66 (2.03)	18.14 (3.12)	17.97 (5.22)

Column header spanning: Aerosol Size

*
The particle removal rate for the smallest size range (0.3–0.5 μm) can be taken as a good approximation to the air changes per hour (ACH).

Table 4.

Average particle removal rate by control type under static and dynamic conditions.

Condition No.	No. of Observations	0.3–0.5 μm * Mean (SD)	0.5–1.0μm Mean (SD)	1.0–3.0μm Mean (SD)	3.0–5.0μm Mean (SD)	5.0–10.0μm Mean (SD)
					Aerosol Size	
Removal rate (hr⁻¹) under static conditions						
Recirculation ratio 90:10	95	8.98 (4.29)	11.42 (6.68)	13.35 (6.31)	13.93 (8.75)	13.89 (9.34)
Recirculation ratio 67:33	97	8.60 (3.47)	10.81 (4.00)	13.19 (4.60)	12.67 (6.24)	11.84 (7.01)
MERV8 filter	146	7.24 (1.94)	9.10 (2.21)	11.44 (3.42)	11.82 (6.01)	11.96 (7.70)
MERV13 filter	46	13.70 (4.45)	17.50 (7.57)	19.06 (2.67)	17.96 (9.95)	15.71 (9.48)
Air purifier	92	8.83 (4.05)	11.32 (6.56)	13.11 (5.67)	12.75 (7.15)	12.51 (8.58)
No air purifier	100	8.74 (3.77)	10.92 (4.30)	13.42 (5.36)	13.79 (7.98)	13.18 (8.04)
Removal rate (hr⁻¹) under dynamic conditions						
Air purifier – High	40	8.56 (1.14)	10.38 (1.27)	12.93 (1.84)	17.48 (5.40)	19.15 (7.38)
Air purifier – Low	20	7.73 (0.75)	8.92 (1.23)	10.77 (2.76)	16.17 (5.44)	16.17 (5.77)
No air purifier	40	9.38 (1.39)	11.55 (1.54)	13.53 (2.00)	16.32 (5.32)	15.50 (5.90)

*
The particle removal rate for the smallest size range (0.3–0.5 μm) can be taken as a good approximation to the air changes per hour (ACH).

Table 5.

F-test results of ANOVA for ACH by particle size range under static and dynamic conditions.

Control type	Aerosol size range [a]				
	0.3–0.5 μm	0.5–1.0 μm	1.0–3.0 μm	3.0–5.0 μm	5.0–10.0 μm
Static conditions					
Recirculation ratio	0.39	0.35	0.84	0.22	0.08 *
Filter MERV rating	0.00 ***	0.00 ***	0.00 ***	0.00 ***	0.00 ***
Air purifier presence	0.84	0.51	0.64	0.30	0.54
Dynamic conditions					
Air purifier presence	0.02 **	0.00 ***	0.08	0.83	0.87
High vs No fan	0.29	0.13	0.85	1.00	0.99
Low vs No fan	0.02 **	0.00 ***	0.08	0.87	0.92
High vs Low fan	0.17	0.06 *	0.18	0.84	0.87

*** $p < 0.01$

** $p < 0.05$

* $p < 0.1$

[a] Each size range had 192 observations under static conditions (n = 192) and 12 observations under dynamic conditions (n = 12).

Author Manuscript Author Manuscript Author Manuscript Author Manuscript

Table 6.

Coefficients of mixed-effects linear regression under static and dynamic conditions.

Control type	Aerosol size range				
	0.3–0.5 μm Coeff. (SE)	0.5–1.0 μm Coeff. (SE)	1.0–3.0μm Coeff. (SE)	3.0–5.0μm Coeff. (SE)	5.0–10.0μm Coeff. (SE)
Static conditions					
Recirculation ratio	0.15 (0.62)	0.09 (0.92)	−0.64 (1.00)	−0.0003 (1.59)	0.04 (1.82)
Filter MERV rating	5 59 *** (0.89)	6.75 *** (1.32)	6.70 *** (1.44)	3.04 (2.28)	1.04 (2.61)
Air purifier presence [a]	0.46 (0.63)	0.47 (0.94)	−0.32 (1.02)	−1.17 (1.62)	−2.30 (1.85)
High Constant	7.06 *** (0.43)	9.04 *** (0.63)	11.86 *** (0.69)	12.47 *** (1.10)	12.53 *** (1.26)
Residual	7.26 (0.74)	16.08 (1.64)	19.10 (1.95)	48.06 (4.90)	63.02 (6.43)
Dynamic conditions Air purifier presence					
High	−1.13 (0.61)	−1.68 ** (0.66)	−0.85 (1.35)	0.27 (3.40)	0.57 (4.05)
Low	−2.53 *** (0.61)	−3.77 *** (0.66)	−3.89 ** (1.35)	−1.96 (3.40)	−1.80 (4.05)
Constant	10.26 *** (0.43)	12.70 *** (0.47)	14.66 *** (0.95)	18.14 *** (2.40)	17.97 *** (2.87)
Residual	0.75 (0.31)	0.88 (0.36)	3.63 (1.48)	23.13 (9.44)	32.85 (13.41)

***
$p < 0.01$

**
$p < 0.05$

*
$p < 0.1$.

[a] The air purifier was only used on the "high fan" setting.